Nanocomposites

A comparison between micro- and nanocellulose-filled composite adhesives for oil paintings restoration

Annalisa Cataldi[1], Lars Berglund[2], Flavio Deflorian[1], and Alessandro Pegoretti*[1]

[1]Department of Industrial Engineering, University of Trento, via Sommarive 9, 38123 Trento, Italy
[2]Department of Fiber and Polymer Technology, Wallenberg Wood Science Center, KTH Royal Institute of Technology, SE-100 44 Stockholm, Sweden

Abstract Cellulose nanocrystals (CNC) and microcrystals (CMC) were selected as reinforcing fillers for poly(2-ethyl-2-oxazoline), a water-soluble thermoplastic adhesive widely used in the restoration of oil paintings. Thin composite films containing 5, 10, and 30 wt% of CNC or CMC were produced by solution mixing and casting. UV-vis spectroscopy showed how CNC preserved the adhesive transparency even at the highest CNC content, while for CMC, a progressive loss of transparency was observed. Thermal analysis evidenced a progressive increase of the glass transition temperature of the polymer matrix induced by CNC, while no effects were observed for CMC. Both micro- and nanocellulose were able to improve the elastic modulus and reduce the thermal expansion coefficient and creep compliance of the adhesive, with effects more pronounced for CNC nanoparticles. Finally, single-lap shear test on bonded ancient oil painting substrates confirmed the improved dimensional stability of the joint imparted by CNC in the adhesive under both quasi-static and creep conditions.

Keywords Cellulose, Nanocomposites, Mechanical properties, Adhesion, Cultural heritage

Introduction

The restoration of oil paintings on canvas, involving various constituting components such as textile substrates, preparation layers, paint films, and varnish layers, is a major concern for conservators.[1] Often, the critical component of oil paintings decay is the substrate. In fact, flax canvas, which is the textile mostly used as a substrate to paint, is sensitive to the microclimate parameters and especially to the humidity level of the exposure environment.[2] Moreover, oil paintings are fixed to a stretcher and therefore subjected to long-lasting tensile stresses. Excessive dimensional variations of canvas and high stretching can promote the deformation of the substrate and, consequently, the formation of cracks in the textile and in the paint film as well, until the separation of the paint from the preparation and the support.[3] In these case, a loss of tension and relaxation of the canvas can be observed.[4] To restore a degraded canvas to its initial mechanical performance, conservators generally follow two strategies: i) the consolidation of the original support and/or ii) the lining of the canvas.[5] In both restoration operations, an adhesive is applied to the damaged textile. In particular, thermoplastic heat-seal adhesives are the mostly used for their good physical properties and high chemical and yellowing stability.[6,7] This research group extensively studied the possibility offered by microcrystalline cellulose to improve the thermomechanical properties of a methylacrylate/ethylene methylacrylate copolymer (Paraloid B72) widely used for the preparation and conservation of cultural heritages.[8–11]

Aquazol 500, a poly (2-ethyl-2-oxazoline), is another versatile adhesive introduced in the field of conservation in the 1990s for its high transparency, good flexibility, and easy removability, being a water soluble polymer, and therefore widely used in the restoration of oil paintings.[12,13] Considering the specific mechanical performance required to an oil paintings adhesive, such as a good dimensional stability and a high resistance to long-lasting stresses, and the well-known reinforcing properties of cellulose-based fillers on polymers,[14–17] this work proposes the application of the composite technology to artwork restoration issues. In particular, considering the recent attention of composite scientists toward cellulose-based fibers reinforcements as renewable alternative to their synthetic equivalents, cellulose microcrystals (MCC) and nanocrystals (CNC) were chosen as fillers in this work.

Moreover, cellulose is also one of the main components of the linen used in ancient oil painting substrates and the usage of similar materials as consolidants should be preferred. On the basis of the promising results obtained by melt-compounded composites based on Aquazol 500 filled with a microcrystalline cellulose,[18] the characterization of micro- and nanocomposites made by solution mixing and casting, using the same thermoplastic polymer and adding a commercial microcellulose and cellulose nanocrystals suspensions, was performed. The comparison between micro- and nanocomposites was

*Corresponding author, email alessandro.pegoretti@unitn.it

Received 21 August 2015; accepted 2 November 2015
DOI 10.1080/20550324.2015.1117239

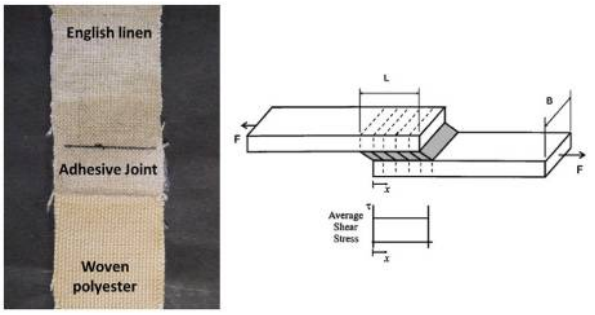

Figure 1 *a* **Representation of an adhesive joint with textile adherents for single-lap shear tests.** *b* **Schematic of testing conditions**

investigated. The main aim of this research is the improvement of the mechanical behavior of a commercial artwork adhesive, especially in terms of creep resistance and adhesive displacement, without impairing the good optical features of this resin, thanks to the use of nanoscale cellulose particles.

Experimental details

Materials

A poly (2-ethyl-2-oxazoline) with the trade name Aquazol 500 (AQ500) by Polymer Chemistry Innovation (USA), with a specific density of 1.07 g cm^{-3} and a molecular weight of 500 kDalton was used as polymeric matrix for micro- and nanocomposites. Cellulose microcrystals (CMC; Sigma Aldrich, USA), with a specific gravity of 1.56 g cm^{-3}, were selected as reinforcing filler. Aqueous suspensions at 5.5–8.7 wt% of cellulose nanocrystals (CNC), produced through the sulfuric acid (64 wt%) hydrolysis of microcrystalline cellulose powder (CMC), were used as nanofiller.[19] According to scanning electron microscopy (SEM) observations (Fig. 2*a* and *b*), CMC particles are elongated flakes with an average length of about 24 μm, a width of about 10 μm, and an average L/D ratio of 2.4, while CNCs are rod-like particles, 100–400 nm long, 5–10 nm wide, with an average aspect ratio of 50.

Samples preparation

Thin films of CMC- and CNC-filled composites with an average thickness of 250 μm and a filler content of 5 wt%, 10 wt% ,and 30 wt%, were obtained by solution mixing and casting. All samples were dried in a vacuum oven at 40 °C until the total solvent evaporation. Before testing, samples were dried at 50 °C for 24 h in a vacuum oven. Samples were denoted indicating the matrix (AQ500), the type of filler (CNC or CMC), and its weight amount. For instance, AQ500-CNC-5 identifies a composite filled with a CNC amount of 5 wt%.

Testing methods

Microstructural observations on cryofractured surfaces of the neat matrix and the corresponding micro- and nanocomposite samples were carried out by a Zeiss Supra 40 high resolution field emission scanning electron microscopy (FESEM) microscope with an accelerating voltage of 1 kV and a beam aperture of 20 μm.

Relative transmittance of the neat matrix and relative composites was determined with a Jasco570 UV-vis-NIR spectrophotometer, at a spectral wavelength range of 250–800 nm.

Thermogravimetric analysis (TGA) was conducted through a Mettler TG50 thermobalance, in a temperature interval between 40 °C and 700 °C, heating rate of 10 °C min^{-1} in a nitrogen flow of 150 ml min^{-1}. The onset temperature (i.e. the temperature associated to a mass loss of 5 wt%) and the residual mass at 700 °C were determined. The maximum degradation temperature was evaluated from the peak of the mass loss rate curve.

The glass transition temperatures (T_g) of CMC and CNC composites were evaluated as the inflection point in the differential scanning calorimetry (DSC) traces, obtained by a Mettler Toledo TC15 calorimeter. Samples of about 12 mg were analyzed under a nitrogen flow of 150 ml min^{-1}. A first heating stage from 0 °C to 120 °C was performed and linked to a cooling stage from 120 °C to 0 °C followed by a second heating stage from 0 °C to 120 °C. All DSC scans were performed at a rate of 10 °C min^{-1}.

Dynamic mechanical thermal analysis (DMTA) was performed by a TA Instruments DMA Q800 device under tensile configuration on rectangular specimens, 15-mm long, 5-mm wide, and 0.25-mm thick. The thermograms of the storage modulus (E′), loss modulus (E″), and loss tangent (tanδ) were measured in a temperature range between −10 °C and 150 °C, at a heating rate of 3 °C min^{-1} and a frequency of 1 Hz. The strain amplitude was fixed at 0.05%, in order to assure a linear viscoelastic behavior. From the slope of the thermal strain

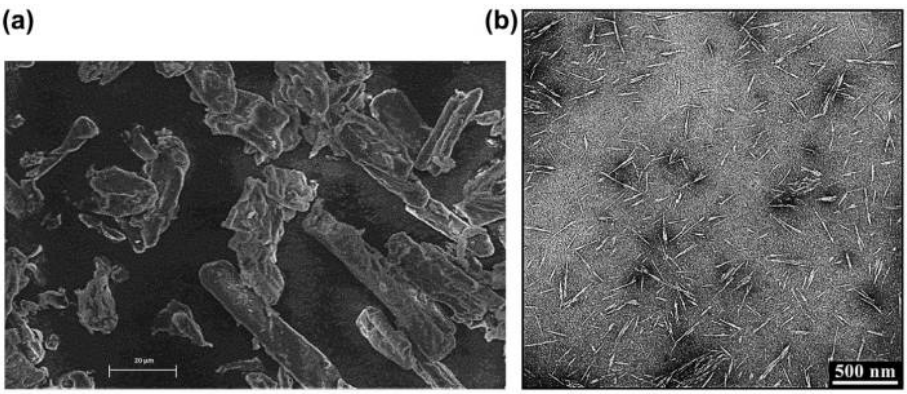

Figure 2 **SEM images of** *a* **micro (CMC) and** *b* **nano (CNC) fillers (courtesy of Dr. Salajkova)**

curves, it was possible to determine the coefficients of linear thermal expansion (CLTE) below T_g (i.e. in a temperature interval between 0 °C and 40 °C) and above T_g (between 60 °C and 80 °C).

Creep tests were conducted by the DMA Q800 device under tensile configuration at 30 °C, applying a constant stress (σ_0) of 4.1 MPa, corresponding to about 10% of the stress at break of the neat AQ500, for a total testing time of 3600 s. Rectangular specimens (15-mm long, 5-mm wide, and 0.25-mm thick) were tested, and the creep compliance D(t) was determined as the ratio between the time-dependent deformation $\varepsilon(t)$ and the applied stress (σ_0). The ratio between the composites values and the neat matrix values of D (i.e. the relative property trend D/D_0) as the function of the filler content was examined.

In order to simulate the consolidation of an ancient oil painting substrate by the canvas lining, single-lap adhesive joints (12.7-mm long and 25-mm wide) connecting two kinds of canvas were prepared. Two types of canvases were selected for this investigation: 1) a pure linen fabric, English canvas, made of boiled and wet spun flax yarn, with an areal weight of 170 g/m^2, an average thickness of 0.35 mm, a yarn count of 22 x 20, and a railroaded pattern, representing the original oil painting canvas; 2) an uncoated woven polyester, Sintel, with an areal weight of 260 g/m^2, an average thickness of 0.45 mm, a yarn count of 22 x 22, and a railroaded pattern, utilized as lining textile. Rectangular samples 200-mm long and 25-mm wide were cut and single-lap shear joints (Fig. 1*a* and *b*) were prepared with both filled and unfilled adhesives at 60°C under a pressure of 1 MPa for 5 min. Before testing, all samples were conditioned for 48 h in a chamber with a super-saturated solution of $Mg(NO_3)_2{\cdot}6H_2O$ at 23 °C and relative humidity of 55%.

Single-lap shear tests in quasi-static and creep conditions were carried out by an Instron® 4502 universal testing machine, equipped with a 10 kN load cell, using a crosshead speed of 10 mm/min to determine the adhesive shear strength (τ_B), calculated as the ratio between the maximum force and the overlapping area. The joint displacement (u) was monitored under a constant stress (τ_0) corresponding to about 50% of the shear stress at break (τ_B) of the samples prepared with the neat matrix adhesive. Creep tests on joints were performed at a temperature of 30 °C and a duration of 3600 s. At least five specimens were tested for each sample and each condition.

Results and Discussions

Microstructure and optical transparency

The dispersion degree of cellulose micro- and nanocrystals within the matrix was evaluated trough FESEM observations of cryofractured surfaces of the neat matrix and the corresponding composites. FESEM images of formulations filled with CMC and CNC are showed in Fig. 3*a* and *b*, respectively. CMC-filled samples with lower filler amounts show how microcellulose particles are uniformly dispersed into the films without any preferential orientation and any significant agglomeration phenomena (Fig. 3*a*). In the enlarged pictures of each microcomposites section, it is possible to recognize single flakes of CMC with an average size of 20 µm. For samples filled with 30 wt% of CMC, a deposit phenomenon of the microfiller is noticed, probably occurred during the solvent clearing, showing that 30 wt% of CMC for this kind of composite processing is too high concentration and leads to accumulation of CMCs at the bottom of samples (Fig. 3*a*). In CNC composites, no agglomeration of nanoparticles is observed. The cryofractured surfaces of these compositions have similar appearance to that of the neat matrix (Fig. 3*b*). Actually, Fig. 3*c* highlights the good stability of nanocellulose crystals in aqueous polymeric solutions, showing CNCs homogeneously dispersed within the matrix even at the highest amount of filler without significant aggregates. The image analysis of the size of these particles through Image J reports a CNC's length of 100–500 nm and a width of 10–50 nm.

Good optical properties and, especially, high transparency levels are among the most important features of a polymer to be applied in the cultural heritage restoration. AQ500 has been introduced as adhesive in the conservation of oil paintings, and other art objects, even for its elevated transparency. The addition of a filler in a polymeric matrix can impair its optical features because of the size of the reinforcing agent, the tendency of the filler to aggregate and/or the filler content.[20,21] In Fig. 4*a* and *b*, transmittance (T) spectra of pure AQ500 and corresponding CMC and CNC composites are reported. If the CMC addition leads to a dramatic drop of T proportional to the filler loading, the introduction of CNCs even at the highest filler amounts has no significant effect on the transmittance of the neat adhesive, especially, in the visible wavelengths interval (400–800 nm). The advantage of the use of CNC instead of CMC clearly emerges if the ratio between the composites values and the neat matrix values of T (i.e. the relative property trend T/T_0) are compared (Fig. 4*c*) as a function of filler content. Even after the addition of 30 wt% of nanocellulose, AQ500 maintains its initial T values, while the corresponding CMC composite is almost completely opaque.

Thermal properties

Thermal properties of all composites films are summarized in Table 1. CMC-filled formulations register a progressive decrease in the onset temperature as the filler content increases due to the lower thermal stability of the microcellulose with respect to AQ500.[22] The decrease in the matrix thermal stability, evident in the reduction in the maximum degradation temperature, T_{MAX}, is already observed at 10 wt% of CMC. A more relevant shift of the onset temperatures toward lower values is shown by all CNC-filled films as the filler loading increases (Table 1) and it is related to the hemicellulose and α-cellulose degradation that anticipates the degradation step of nanocellulose.[23,24] Although the thermal stability of CNC is lower than the pure matrix, with a range of degradation temperatures centered between 250 and 400 °C,[25] all compositions with 5 wt% and 10 wt% of nanofiller register just a slight decrease in the maximum degradation temperature, T_{MAX}, while samples with the highest amount of CNC show a reduction of about 10% of this property. This evidences that a CNC amount of 30 wt% is quite critical for the matrix, in terms of degradation resistance. In particular, at the higher presence of CNCs, the stronger influence of the main degradation peak of this filler centered at about 350 °C[23,24] shifts the T_{MAX} of AQ500 towards the CNC main degradation temperature. Moreover, the residual mass at 700 °C increases proportionally to the filler content in all formulations and this phenomenon is more

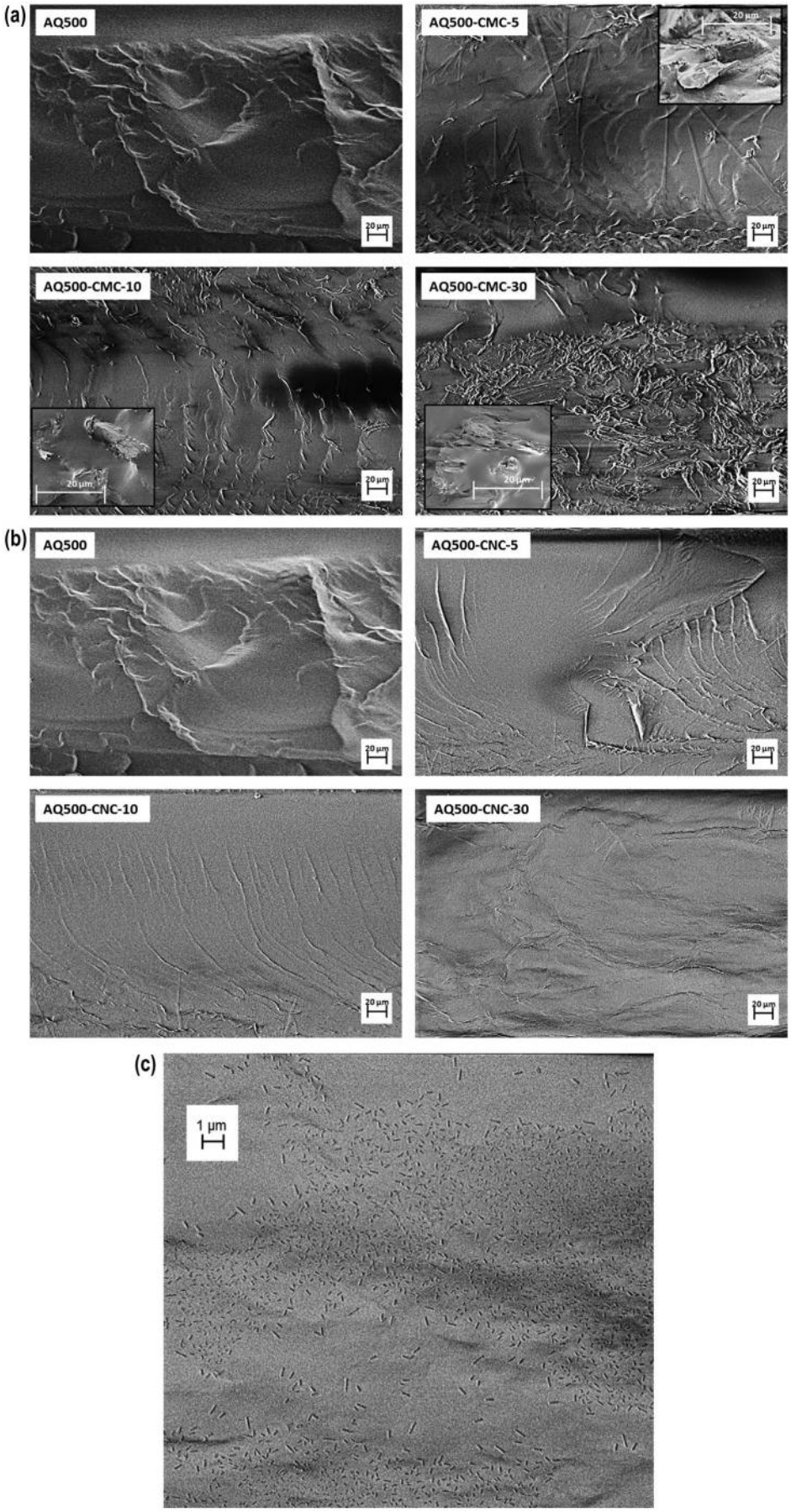

Figure 3 SEM images of thin adhesive films: *a* **CMC composites;** *b* **CNC composites;** c **higher magnification of the cryofractured surface of Aquazol 500 filled with 30 wt% of CNC.**

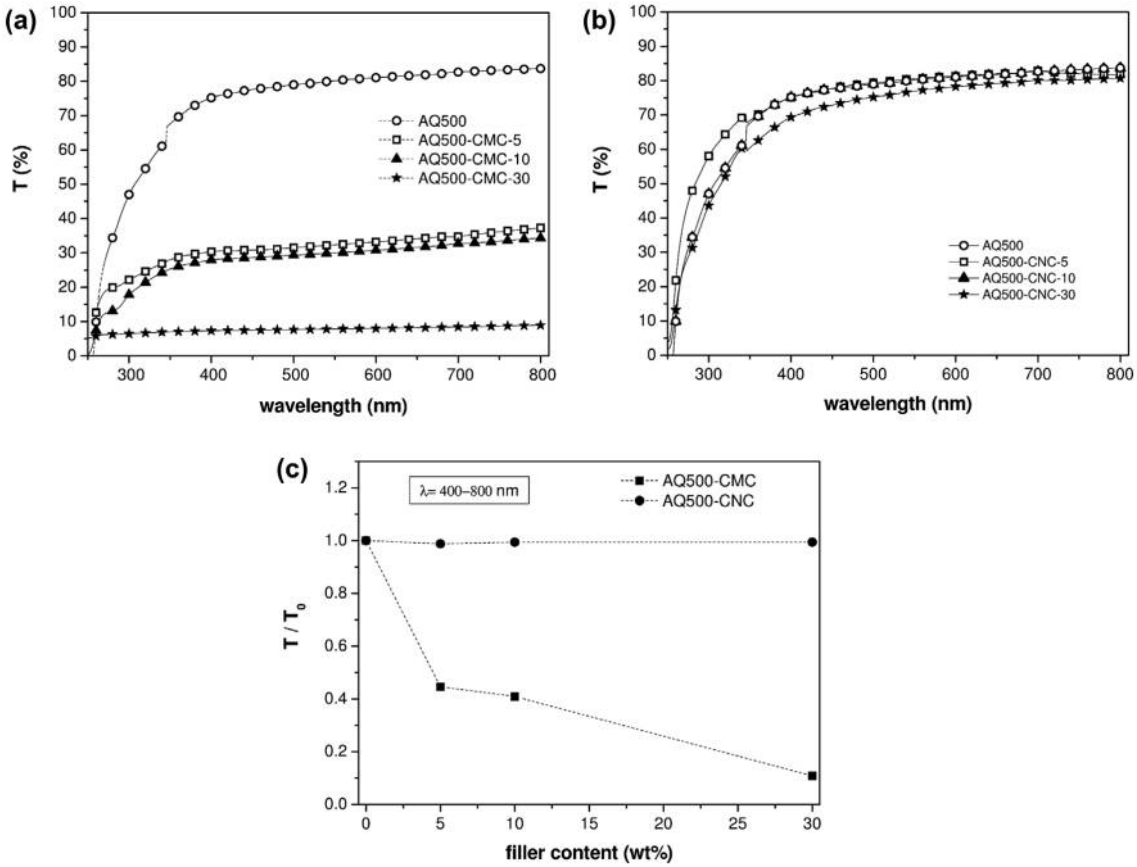

Figure 4 UV-vis spectroscopy results: *a* **transparency (T) of neat AQ500 and corresponding microcomposites;** *b* **transparency (T) of neat AQ500 and corresponding nanocomposites;** *c* **relative transparency (T/T_0) values in the visible wavelengths range as a function of the filler content of micro- (AQ500-CMC) and nanocomposites (AQ500-CNC)**

Table 1 Results of TGA tests on neat AQ500 and relative nano- and microcomposites

sample	T_{onset}*(°C)	T_{max}**(°C)	Residual mass at 700 °C (%)
AQ500	364	416	–
AQ500-CMC-5	313	418	–
AQ500-CMC-10	276	405	0.30
AQ500-CMC-30	267	403	3.91
AQ500-CNC-5	271	410	–
AQ500-CNC-10	238	409	1.10
AQ500-CNC-30	198	367	4.45

*T_{onset} = temperature of the initial degradation step (corresponding to a mass loss of 5 wt%).
**$T_{max=}$temperature of the maximum degradation rate.

evident in composites samples made of CNC suspensions. As well known in the literature, sulfate groups, present on the surface of CNCs, allow the formation of a ceramized surface layer on the samples that acts as flame retardant, impeding the complete combustion and vaporization of the matrix.[26] Considering DSC results (Table 2), all formulations report an increase in the glass transition temperature T_g, in the second heating stage, while just CNC suspensions provide the increase in the T_g of the neat matrix even in the first heating stage. The nanosize of CNC makes it more able to interact with polymeric chains of AQ500 and modify their mobility. The viscoelastic properties of unfilled AQ500 and CMC and CNC composites are listed in Table 3, while the representative DMTA thermograms of compositions filled with CMC and CNC are showed in Fig. 5*a* and *b*. Both CMC and CNC produce a remarkable increase in storage and loss moduli (E′ and E″), proportional to the filler content. Correspondingly, loss factor (tan δ) values decrease as the filler amount increases in all formulations (Table 3). Also, DMTA analysis proves the more powerful action of CNCs on the AQ500 glass transition temperature, with a progressive enhancement of this property, determined from the shift of the E″ peak toward higher temperatures. While for CMC compositions, no significant effect on the T_g is detected. Interestingly, CMCs and CNCs promote the improvement of the dimensional stability of the neat adhesive as one can see in the reduction in the CLTE below and above T_g (Table 3) as the filler content increases, registered by the two groups of composites. Additionally, the ratios between the composites values and the neat matrix values of E′, E″, T_g, and CLTE in the glassy state (i.e. the relative properties trends E'/E'_0, E''/E''_0,

Table 2 Glass transition temperatures (T_g) of neat AQ500 and relative micro- and nanocomposites from DSC tests (first and second heating stage)

Sample	T_g (°C)	
	First heating	Second heating
AQ500	44.1	55.7
AQ500-CMC-5	44.4	62.2
AQ500-CMC-10	45.4	61.7
AQ500-CMC-30	44.8	62.0
AQ500-CNC-5	55.4	59.4
AQ500-CNC-10	56.5	59.0
AQ500-CNC-30	57.1	61.3

Table 3 Results of DMTA tests on neat AQ500 and relative micro- and nanocomposites

Sample	E'at 25 °C(GPa)	E"peak value(GPa)	tanδpeak value	T_g at E" peak(°C)	$CLTE_g(K^{-1})$	$CLTE_r(K^{-1})$
AQ500	1.86	0.41	3.21	72.0	8.9E-05	8.7E-03
AQ500-CMC-5	2.53	0.53	2.16	69.1	9.0E-05	3.9E-03
AQ500-CMC-10	3.55	0.69	1.81	68.9	6.0E-05	3.5E-03
AQ500-CMC-30	4.60	0.96	0.84	68.9	3.5E-05	6.7E-04
AQ500-CNC-5	3.06	0.70	2.23	74.7	5.9E-05	4.2E-03
AQ500-CNC-10	3.72	0.82	1.88	77.1	3.9E-05	3.5E-03
AQ500-CNC-30	6.86	1.33	0.78	82.6	1.0E-05	3.3E-04

E': storage modulus at different temperatures.
Tg: glass transition temperature.
$CLTE_g$: coefficient of linear thermal expansion in the glassy state (interval 0 °C–40 °C).
$CLTE_r$: coefficient of linear thermal expansion in the rubbery state (interval 70 °C–80 °C).

and $CLTE_g/CLTE_{g0}$) as the function of the filler content were investigated. The comparison between the relative trends of E', Tg, and CLTE in the glassy and rubbery states of CMC and CNC composites as a function of filler content is reported in Figure 6*a–c*. Although both fillers produce similar trends for E' and CLTE, it is evident that CNCs provide stronger effects than CMC flakes. Formulations with 30 wt% of CNC suspensions reach E' values three times higher than the neat AQ500 (Fig. 6*a*) and register a thermal expansion reduction of about 90% in comparison to CLTE values of microcomposites that are 40% lower than the neat adhesive (Fig. 6*c*). Only CNC is able to modify the T_g of the neat Aquazol, see Fig. 6*b*.

Mechanical response

The stabilizing effect due to the introduction of CMC and CNC within AQ500 is highlighted also in the creep tests, where a decrease in the creep compliance (D) of all filled adhesive films is detected (Fig. 7*a*). Again the CNC effect on the improvement of the constant stress response are more pronounced than for CMC. CMC-filled films, after a testing time of 3600 s, can reduce D by up to 60% compared with the neat matrix; CNC films can show a 90% reduction in D. This is a very important result, considering the end use of AQ500 in the field of cultural heritage conservation as a consolidant/adhesive for oil paintings, which being fixed to a stretcher, are subjected to long-lasting constant stresses. In order to prove that this positive stabilization of the matrix promoted by CMCs and CNCs is also active during the application of AQ500 as canvas consolidant/adhesive, single-lap shear tests in quasi-static and creep conditions were performed on adhesive joints based on CMC and CNC composites (Fig. 1).

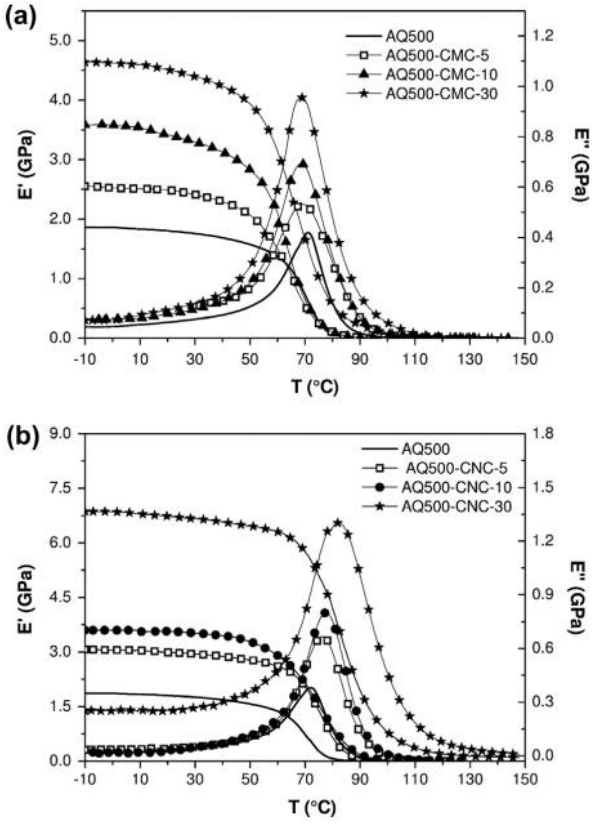

Figure 5 Representative DMTA thermograms: *a* **CMC composites;** *b* **CNC composites**

The adhesive strength (τ_B) and the joint displacement values of the neat matrix and the relative micro- and nanocomposites are listed in Table 4. Cellulose micro- and nanocrystals

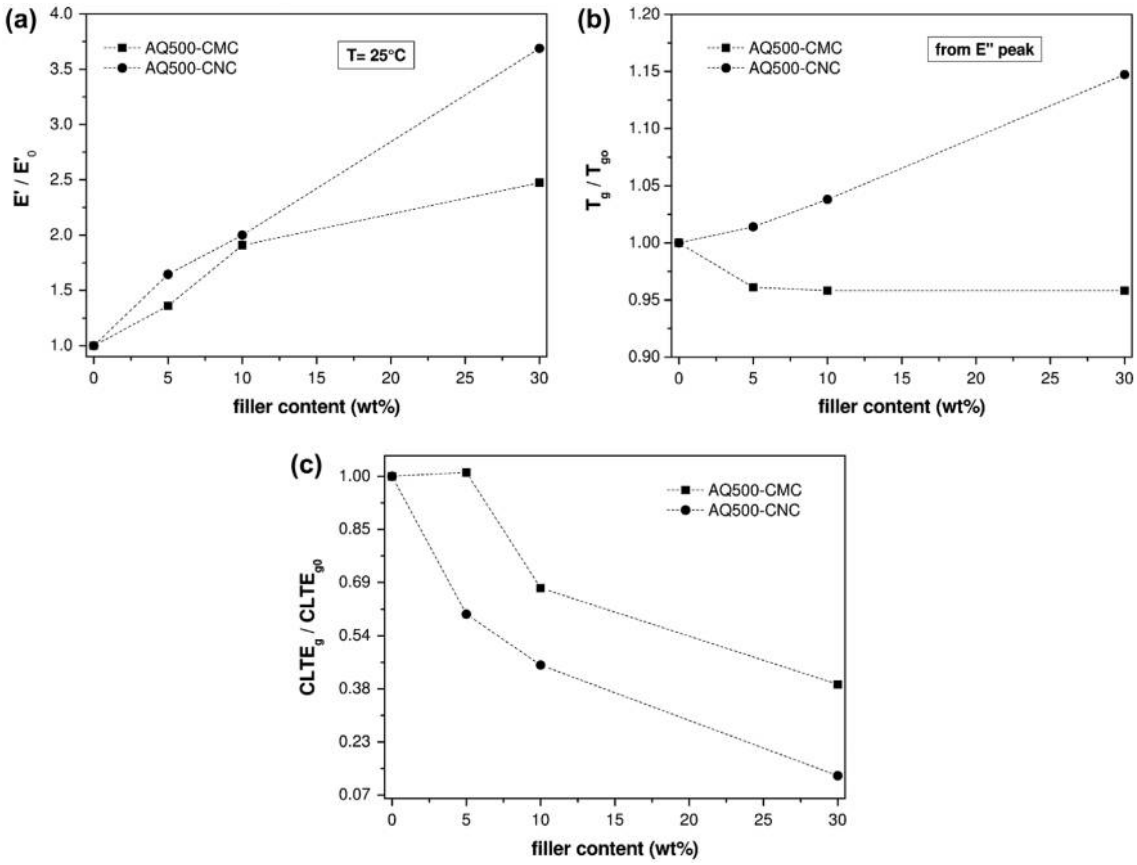

Figure 6 Main results from DMTA analysis: *a* **relative storage modulus;** *b* **relative glass transition temperature;** *c* **relative coefficient of linear thermal expansion below T_g of micro- (AQ500-CMC) and nanocomposites (AQ500-CNC)**

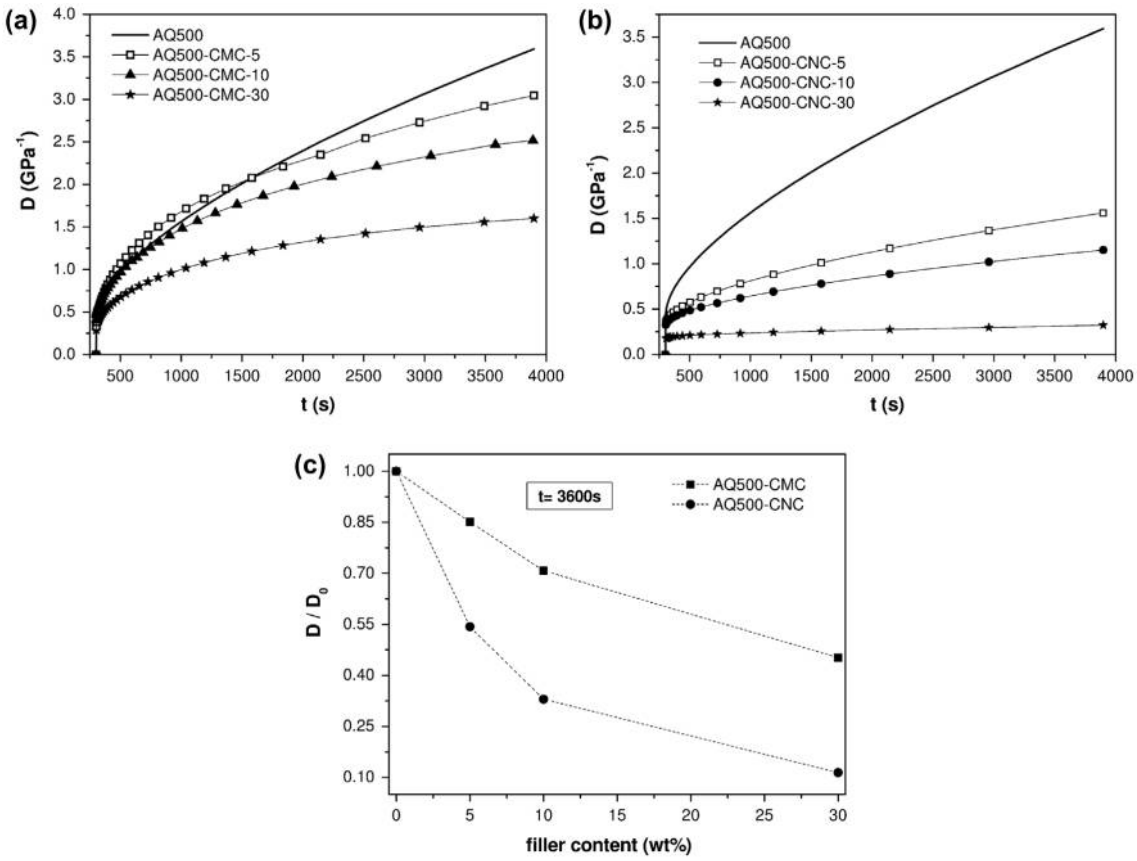

Figure 7 Main results from creep tests: *a* **representative creep compliance curves (D) of neat AQ500 and corresponding microcomposites;** *b* **representative creep compliance curves (D) of neat AQ500 and corresponding nanocomposites;** *c* **relative creep compliance values at 3600 s of micro- (AQ500-CMC) and nanocomposites (AQ500-CNC)**

Table 4 Results of single-lap shear tests on the neat matrix and relative micro- and nanocomposites

Sample	τ_B(MPa)	uat t= 3600s (mm)
AQ500	2.87 ± 0.02	19.71 ± 0.03
AQ500-CMC-5	2.51 ± 0.01	15.68 ± 0.03
AQ500-CMC-10	2.47 ± 0.02	14.15 ± 0.02
AQ500-CMC-30	1.30 ± 0.04	–
AQ500-CNC-5	2.70 ± 0.02	11.13 ± 0.02
AQ500-CNC-10	2.63 ± 0.05	9.11 ± 0.02
AQ500-CNC-30	2.00 ± 0.02	7.29 ± 0.04

τ_B: shear strength.
u: joint displacement.

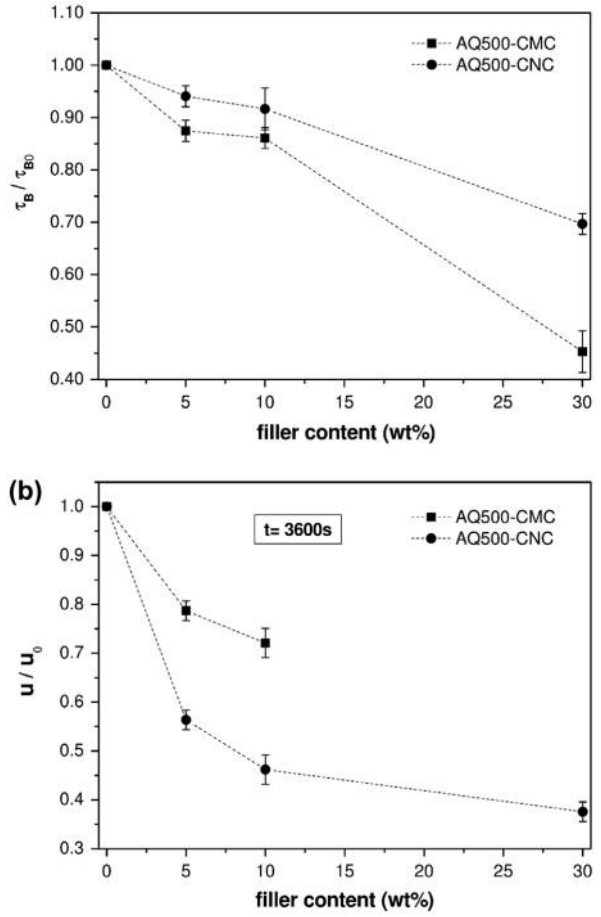

Figure 8 Trends of relative single-lap shear tests properties of adhesive joints based on CMC and CNC polymer composites: *a* adhesive strength (τ_B); *b* joint displacement (u)

lead to a decrease in the adhesive strength of AQ500 related to the filler content, but for CMC-filled adhesive joints, this reduction in τ_B is dramatic at 30 wt% CMC. Data confirm that 30 wt% of CNC and especially of CMC is a maximum filler content for the present materials. On the other hand, a systematic reduction in the adhesive displacement u is observed even at the lowest amount of filler, in particular for CNC (Table 4). In order to better visualize the situation, the ratios between the composites values and the neat matrix values of τ_B and u (i.e. the relative properties trends τ_B/τ_{B0} and u/u_0) as the function of the filler content were evaluated and reported in Fig. 8*a* and *b*. The joint strength is impaired by both CMC and CNC, even if with different trends. The most likely explanation is a decrease in the adhesive properties of the filled samples due to cellulose aggregates initiating premature failure possibly combined with insufficient adhesion levels between the adhesive and the filler. The strength reduction up to a filler content of 10 wt% is acceptable for the final application. It was not possible to perform single-lap shear tests under creep condition on microcomposites at 30 wt% of CMC since they failed during tests, since the shear stress used for these tests ($\tau_{0=}$50% of the AQ500 τ_B value) is higher than their actual strength. On the other hand, one can notice that microcomposites manifest a positive reduction in the creep displacement of up to about 30% for formulations with 10 wt% of CMC. Concurrently, formulations filled with CNC suspensions reach u values up to 60% lower than the neat matrix, thus indicating a superior stabilizing effect of CNC over CMC.

Conclusions

The physical and thermomechanical properties of thin adhesive films made of a thermoplastic adhesive (AQ500) used for artwork restoration and various amounts of both CNC and CMC were investigated. All nanocomposites preserved their high transparency even at high amounts of CNC, while CMC flakes impaired the optical features of the neat matrix with increasing content of the CMC filler. Only CNC was able to improve the glass transition temperature of the pure polymer but for formulations with the highest amount of CNC, a high decrease in the thermal stability was detected. Both micro- and nanocellulose promoted a stabilizing effect on the neat matrix with increased storage modulus and reduced thermal expansion coefficient and creep compliance with increasing filler content. Interestingly, CNC was significantly more effective than CMC in improving the viscoelastic and mechanical response. This is related to the better mechanical properties of CNC and more efficient load-carrying capabilities due to its higher aspect ratio. This positive action was observed also during single-lap shear tests. Although CNC films showed a decrease in the adhesive shear strength at the highest filler contents, a significant reduction in the adhesive displacement since the lowest filler loading under creep conditions was detected.

Conflict of interest

The authors have no conflicts of interest to declare.

Acknowledgments

Prof. Alberto Quaranta and PhD candidate Walter Raniero for support in UV-vis spectroscopy analysis, Mr Lorenzo Moschini

for assistance with FESEM analysis, and Mrs Lilia Gianotti and Mr Lorenzo Pontalti for supplying canvas textiles are kindly acknowledged. Moreover, the authors wish to thank Dr. Salajkova for courteously providing Fig. 2*b* and Dr. Kasinee Prakobna for her assistance in CNC preparation.

ORCID

Berglund Lars http://orcid.org/0000-0001-5818-2378
Deflorian Flavio http://orcid.org/0000-0002-3849-4988
Pegoretti Alessandro http://orcid.org/0000-0001-9641-9735

References

1 C. Villers: ed. Lining paintings: papers from the greenwich conference on comparative lining techniques, 191, 2004, London, Archetype Publications.
2 G. A. Berger and W. H. Russell: 'Conservation of paintings: research and innovations', 376, 2007, London, Archetype Publications.
3 M. F. Mecklenburg: National Museum, unpublished work, 1982.
4 S. Hackney: *The Conservator*, 1990, **14**, (1), 44–52.
5 P. Ackroyd: *Rev. Conserv.*, 2002, **3**, 3–14.
6 C. F. J. Bria: *WAAC Newsletter*, 1986, **8**, (1), 7–11.
7 G. A. Berger: *J. Am. Inst. Conserv.*, 1978, **18**, (1), 44–45.
8 A. Cataldi, F. Deflorian and A. Pegoretti: *Mater. Des.*, 2015, **83**, 611–619.
9 A. Cataldi, A. Dorigato, F. Deflorian and A. Pegoretti: *J. Mater. Sci*, 2014, **49**, (5), 2035–2044.
10 A. Cataldi, A. Dorigato, F. Deflorian and A. Pegoretti: *J. Appl. Polym. Sci.*, 2014, **131**, (18), 40741, 40741–40746.
11 A. Cataldi, A. Dorigato, F. Deflorian and A. Pegoretti: *Polym. Eng. Sci.*, 2015, **55**, (6), 1349–1354.
12 T. T. Chiu and W. J. Fairchock: 'Poly (2-ethyl-2oxazoline): A new water- and organic-soluble adhesive', in 'Water-soluble polymers: Beauty with performance', (ed. J. E. Glass), 425–433; 1986, Washington, D.C., American Chemical Society.
13 R. C. Wolbers, M. McGinn and D. Duerbeck: 'Poly(2-Ethyl-2-Oxazoline): a new conservation consolidant', AIC-WAG proceedings: Painted Wood: history and conservation, 1994, 514–527.
14 A. Bledzki and J. Gassan: *Prog. Polym. Sci.*, 1999, **24**, 221–274.
15 S. J. Eichhorn, A. Dufresne, M. Aranguren, N. E. Marcovich, J. R. Capadona, S. J. Rowan, C. Weder, W. Thielemans, M. Roman, S. Renneckar, W. Gindl, S. Veigel, J. Keckes, H. Yano, K. Abe, M. Nogi, A. N. Nakagaito, A. Mangalam, J. Simonsen, A. S. Benight, A. Bismarck, L. A. Berglund and T. Peijs: *J. Mater. Sci*, 2010, **45**, (1), 1–33.
16 J. P. F. Lagerwall, C. Schütz, M. Salajkova, J. Noh, J. Hyun Park, G. Scalia and L. Bergström: *NPG Asia Mater*, 2014, **6**, e80.
17 G. Siqueira, J. Bras and A. Dufresne: *Polym.*, 2010, **2**, (4), 728–765.
18 A. Cataldi, F. Deflorian and A. Pegoretti: *Int. J. Adhes. Adhes.*, 2015, **62**, 92–100.
19 A. Pei, Q. Zhou and L. A. Berglund: *Compos. Sci. Technol.*, 2010, **70**, (5), 815–821.
20 J. A. Mbey, S. Hoppe and F. Thomas: *Carbohydr. Polym.* , 2012, **88**, (1), 213–222.
21 B. Yu, H. -N. Lim and Y. -K.Lee: *Mater. Des.*, 2010, **31**, (10), 4719–4724.
22 A. Cataldi, A. Dorigato, F. Deflorian and A. Pegoretti: *J. Mater. Sci.*, 2014, **49**, (5), 2035–2044.
23 E. Abraham, B. Deepa, L. A. Pothan, M. Jacob, S.Thomas, U. Cvelbar and R. Anandjiwala: *Carbohydr. Polym.* , 2011, **86**, (4), 1468–1475.
24 A. Mandal and D. Chakrabarty *Carbohydr. Polym.* , 2011, **86**, (3), 1291–1299.
25 E. Abraham, M. S. Thomas, C. John, L. A. Pothen, O. Shoseyov, and S. Thomas: *Ind. Crop. Prod.*, 2013, **51**, (0), 415–424.
26 M. Roman and W. T. Winter, *Biomacromolecules*, 2004, **5**, (5), 1671–1677.